Medical Dosimetry, Vol. 33, No. 2, pp. 124-134, 2008

0958-3947/08/$–see front matter

doi:10.1016/j.meddos.2008.02.005

USE OF THE BRAINLAB EXACTRAC X-RAY 6D SYSTEM IN IMAGE-GUIDED RADIOTHERAPY

JIAN-YUE JIN, PH.D., FANG-FANG YIN, PH.D., STEPHEN E. TENN, PH.D., PAUL M. MEDIN, PH.D., and TIMOTHY D. SOLBERG, PH.D.

Department of Radiation Oncology, Henry Ford Health System, Detroit, MI; Department of Radiation Oncology, Duke University Medical Center, Durham, NC; Department of Radiation Oncology, David Geffen School of Medicine at UCLA, Los Angeles, CA; and Department of Radiation Oncology, University of Nebraska, Nebraska Medical Center, Omaha, NE

(*Received* 1 *November* 2007; *accepted* 29 *February* 2008)

Abstract—The ExacTrac X-Ray 6D image-guided radiotherapy (IGRT) system will be described and its performance evaluated. The system is mainly an integration of 2 subsystems: (1) an infrared (IR)-based optical positioning system (ExacTrac) and (2) a radiographic kV x-ray imaging system (X-Ray 6D). The infrared system consists of 2 IR cameras, which are used to monitor reflective body markers placed on the patient's skin to assist in patient initial setup, and an IR reflective reference star, which is attached to the treatment couch and can assist in couch movement with spatial resolution to better than 0.3 mm. The radiographic kV devices consist of 2 oblique x-ray imagers to obtain high-quality radiographs for patient position verification and adjustment. The position verification is made by fusing the radiographs with the simulation CT images using either 3 degree-of-freedom (3D) or 6 degree-of-freedom (6D) fusion algorithms. The position adjustment is performed using the infrared system according to the verification results. The reliability of the fusion algorithm will be described based on phantom and patient studies. The results indicated that the 6D fusion method is better compared to the 3D method if there are rotational deviations between the simulation and setup positions. Recently, the system has been augmented with the capabilities for image-guided positioning of targets in motion due to respiration and for gated treatment of those targets. The infrared markers provide a respiratory signal for tracking and gating of the treatment beam, with the x-ray system providing periodic confirmation of patient position relative to the gating window throughout the duration of the gated delivery. © 2008 American Association of Medical Dosimetrists.

Key Words: **Image-guided radiation therapy, X-ray guidance, Image fusion, Respiratory gating.**

INTRODUCTION

Image guidance plays an important role in radiosurgery and intensity modulated radiotherapy (IMRT) because it supports accurate target localization and avoidance of adjacent organs-at-risks (OAR). A number of imaging modalities including: ultrasound,[1,2] video imaging,[3,4] 2-dimensional radiographic imaging (kV and MV),[5–7] computed tomography (CT) (conventional CT as well as kV and MV cone beam CT),[8–12] and magnetic resonance imaging (MRI)[13–15] are used in image-guided radiotherapy (IGRT). Several IGRT systems are now commercially available and have been successfully implemented for clinical applications. The BrainLAB ExacTrac X-Ray 6D stereotactic IGRT system (BrainLAB AG, Feldkirchen, Germany) uses a combination of optical positioning and kV radiographic imaging to accurately position patients and make online positioning corrections. It has been successfully used clinically for intra-cranial and extra-cranial radiosurgery.[16–19] The ExacTrac X-Ray 6D system is mainly an integration of 2 subsystems: (1) an infrared (IR)-based optical positioning system (ExacTrac) for initial patient setup and precise control of couch movement, and (2) a radiographic kV x-ray imaging system (X-Ray 6D) for position verification and readjustment based on the internal anatomy or implanted fiducials. In addition, the IR system can be used to monitor a patient's respiration and provide a signal to the linac for tracking and gating of the treatment beam. Used in conjunction with the x-ray system, image-guided verification of target position relative to the gating window can be performed throughout the duration of the gated delivery. It should be pointed out that besides the IR devices and the x-ray imagers, the system includes a digital video camera for monitoring a patient's position during treatment. In addition, the system software supports an ultrasound module that could replace the radiographic kV x-ray imagers for positioning guidance around soft tissue targets such as the prostate. This article will present a detailed description of the ExacTrac X-Ray 6D system including evaluations of performance and limitations, only for the infrared and x-ray components.

SYSTEM DESCRIPTION

Infrared

The infrared tracking component of the ExacTrac X-Ray 6D system includes 2 IR cameras, passive IR-

Reprint requests to: Jian-Yue Jin, Ph.D., Department of Radiation Oncology, Henry Ford Hospital, Detroit, MI 48202. E-mail: Jjin1@hfhs.org

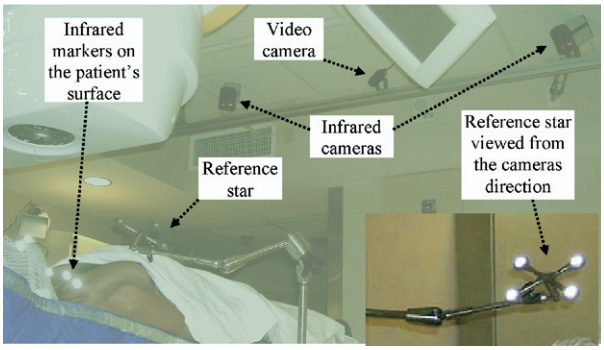

Fig. 1. The infrared camera-based ExacTrac system.

reflecting spheres placed on a patient's surface, and a reference device (the reference star) that contains 4 reflective circles (Fig. 1). The IR cameras are rigidly mounted to a metal bar attached to the ceiling and emit a low IR signal that is reflected and analyzed for positioning information. A 2-step calibration procedure has been established to ensure that the IR cameras can accurately determine the position of IR reflectors in the treatment room. The first step corrects for distortions in the IR system and creates a coordinate space, while the second step provides the system with the location of the linear accelerator (LINAC) isocenter. Studies by Wang *et al.*[20] have demonstrated that the position of each IR-reflecting sphere can be determined to less than 0.3 mm. Automatic setup can then be easily achieved by moving the couch to match the marker's position with those recorded in a CT image. In addition, the software also provides rotational offsets along 3 primary axes. However, the external markers have to be positioned in a relatively stable location to achieve accurate setup. With the use of the reference star attached to the couch, the couch's movement can be precisely determined.

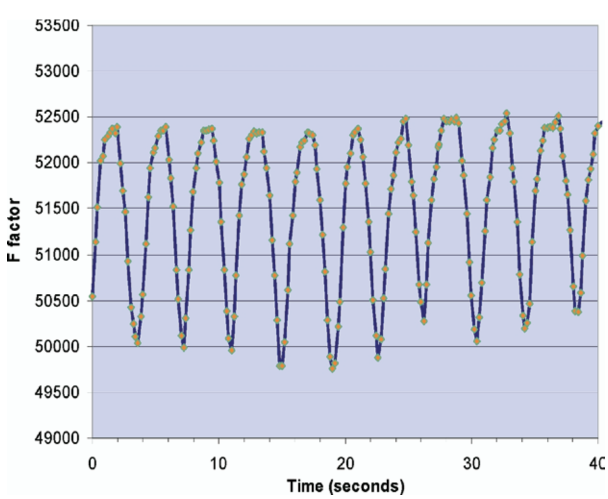

Fig. 2. Respiratory motion from a patient at UCLA, characterized by the 3D F-factor defined by Baroni *et al.* (2000).

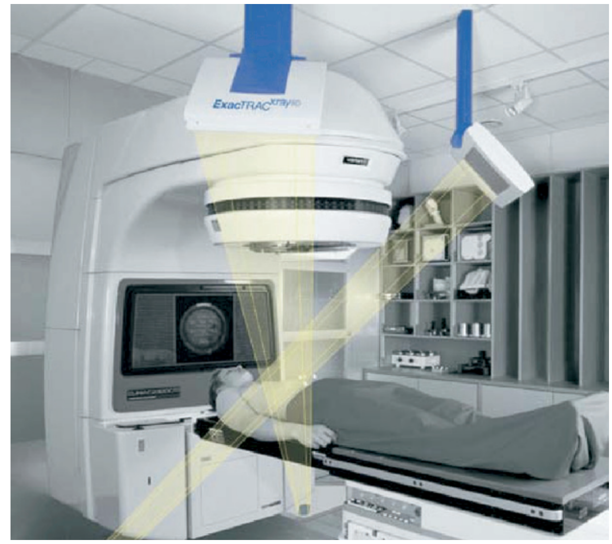

Fig. 3. The Novalis body image-guided system showing oblique configurations of the x-ray imaging devices.

The IR system samples marker positions at a frequency of 20 Hz and therefore may also be used to monitor patient motion. Figure 2 shows an example of a patient's respiratory motion monitored using this system. The y-axis is a 3-dimensional (3D) composite of the combined motion of 5 markers placed on a patient's chest.[21] The system has subsequently been adopted for use in respiratory correlated imaging[22] and gated radiotherapy.[23,24]

X-ray

The x-ray component consists of 2 floor-mounted kV x-ray tubes, projecting medial, anterior, and inferior obliquely into 2 corresponding flat panel detectors mounted on the ceiling (Fig. 3). The configuration of this x-ray system is unique compared to the general diagnostic x-ray systems in that: (1) the x-ray tubes and corresponding detector panels are in fixed positions, (2) the x-rays project in an oblique direction relating to the patients, and (3) the source isocenter and source detector distance is relatively large (2.24 and 3.62 meters, respectively).

Two x-ray images are obtained after a patient is initially setup with the ExacTrac (infrared) system. These images are then compared with the patient's 3-dimensional (3D) CT simulation images with the corresponding isocenter in terms of digital reconstructed radiography (DRR). The software provides several options for matching the images. The manual match and the 3D (3 degrees of freedom) fusion methods assume that the patient was setup with no rotational offsets. Corresponding DRRs are generated at the fixed angles and position adjustment in 3 translational directions (3 degrees of freedom) is performed in the DRRs to best match the x-ray images. Therefore, the manual fusion and 3D fusion use a simple 2D (x-ray) to 2D (DRR) image fusion algorithm. In 2004, the 6D (6 degrees of freedom) fusion option has been clinically implemented. The 6D fusion software first generates various sets of DRRs with position variations in both 3 translational and 3 rotational directions (6 degrees of freedom) for the CT images. It then compares these DRRs with the corresponding x-ray images and obtained the set of DRRs with the maximal similarity to the corresponding x-ray images. The best match is thus determined and the 3 translational and 3 rotational position variations used to generate the set of DRRs are the 6D offsets to fuse the images. Therefore, the 6D fusion method is actually a 2-dimensional (x-ray) to 3-dimensional (CT) image fusion algorithm. It should be pointed out that both 3D and 6D fusion methods have the choice of selecting a region of interest for fusion and can exclude any structures that could potentially increase uncertainty in the fusion. The software also provides a match method of using implanted markers. The patient position accuracy and the amount of offsets can be determined by comparing the implanted markers' position in the x-ray images with those in the CT images. For all of these methods, once the offsets are given, a patient's position can be precisely adjusted using IR guidance. A set of verification x-ray images can be obtained to check the position after readjustment.

The x-ray image fusion-guided position readjustment is usually performed once for each fraction before treatment. Due to the special configuration of the x-ray system, a set of x-ray images can only be obtained when the linac gantry is at around 0°, 80° to 100°, and 260° to 280°. Therefore, monitoring patient position during treatment using the x-ray system is not always possible for many treatment field settings. However, the x-ray image fusion can be performed to readjust position between two fields if position drift is a concern.

Respiratory gating

In 2005, the basic ExacTrac system has been augmented to include a module for image-guided positioning of targets in motion due to respiration and for gated treatment of those targets. The ExacTrac Adaptive Gating system uses stereoscopic kilovoltage radiographs for patient positioning and the IR marker detection system for respiratory tracking and gating of the treatment beam.

Although it may be possible to track lung tumors directly using plane radiography,[25] the ExacTrac Adaptive Gating system is currently designed to be used with radiopaque fiducial markers implanted near the target isocenter.[26–29] These markers are implanted before treatment planning begins and should be placed close enough to the target anatomy so that they can be seen within the field of view of the x-ray localization system at the time of treatment. It is assumed that the spatial relationship between markers and target anatomy will remain relatively fixed.[30] After fiducial markers have been implanted, a CT scan is obtained and a treatment plan is created. The CT planning information is then transferred to the ExacTrac system software. The user locates the fiducials in this CT dataset and their 3D coordinates are used with the pinhole camera model to generate the expected 2D image coordinates for each x-ray imaging detector.

For treatment, a patient is set up in the treatment room and IR reflective markers are attached to the abdomen so that breathing motion can be monitored. The reference star is also used here, both as a reference against which the movement of patient mounted markers is measured, and also to track couch location during the patient positioning process. The 3D movement of the patient's anterior surface is tracked via the IR markers and the anterior-posterior (A-P) component of this trajectory is used to monitor breathing motion. Target position is expected to be correlated with this breathing motion.

The ExacTrac system plots breathing motion vs. time, and a gating reference level is specified on this breathing trace (Fig. 4). The gating level is the amplitude of the breathing trace at which the kV x-ray images for patient localization will be triggered. The images are obtained sequentially at the instant the breathing trace crosses this level during the exhale phase. Because the patient will be localized based on these images, the gating level should be set at the same phase in the breathing cycle at which the planning CT data was obtained. Within each image, the user locates the positions of the implanted fiducials. From these positions, the system reconstructs the 3D geometry of the implants and determines the shifts necessary to bring them into alignment with the implants' orientation as determined from the planning CT. These localization shifts are then made to the patient just as with the basic ExacTrac system. Once the patient has been positioned in this way, the target will pass through the linac isocenter as the breathing trace passes through the gating level.

A high degree of correlation between the breathing trace and internal target motion is important for accurate target coverage. Recent correlation studies have addressed the ability of external surrogates of breathing to predict the position of internal target locations.[27,31–39] Generally, these studies have shown a good degree of correlation but may be dependent on the location of both external markers and internal target. Results of clinical research by Schweikard *et al.*[36] showed that correlation errors less than 2 mm between internal target and external surface motion is possible over treatment times as long as 70 minutes. However, several authors have noted intrafractional changes in the relationship between respiratory signal and tumor position due to unstable breathing.[27,33,37,38] Breathing instruction might be able to improve predictability of tumor location with respect to external respiratory signal, thus increasing treatment accuracy.[40]

Due to the uncertain nature of respiratory surrogate correlation with tumor position, intrafraction verification

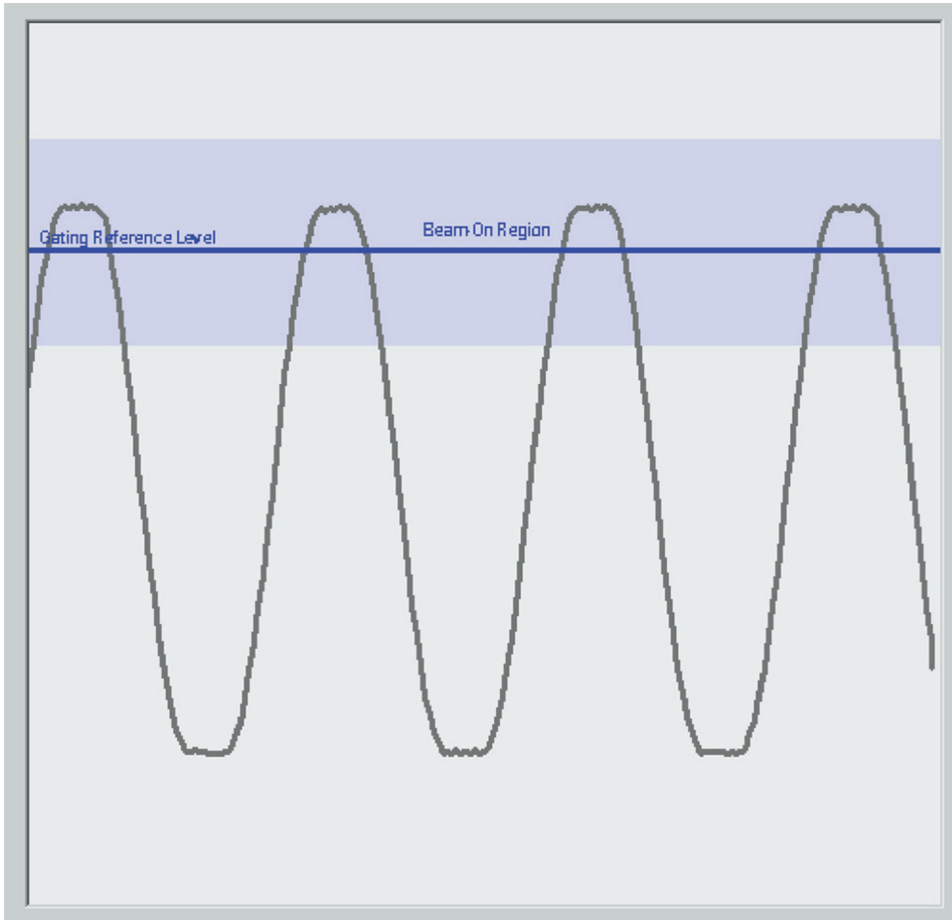

Fig. 4. Breathing trace with gating level (dark line) near 90% and gating window (light band) shown.

of the target position with respect to the respiratory trace is important. Therefore, gated kV x-ray images of the implant marker locations are obtained at the gating level continuously during treatment. However, the treatment will not be interrupted during the acquisition of these images only for those fields in which the LINAC gantry does not block the x-ray. If marker positions remain within tolerance limits, the target position may also be assumed to be correctly positioned. If they are outside the limit, the newly obtained images can be used to reposition the patient and maintain treatment accuracy.

Finally, a gating window (Fig. 4) is determined. The system can gate the beam in both inhale and exhale phases of the breathing cycle; however, the treatment beam is gated during the exhale phase because hysteresis of target motion has been observed during the breathing cycle.[41] Localization is also performed in the exhale phase; therefore, it is expected that the target is most accurately positioned here.

SYSTEM EVALUATION

Phantom studies for localization accuracy

Yan *et al.*[42] had systematically studied the localization accuracy of an earlier version of the ExacTrac X-Ray 6D system in an anthropomorphic phantom. They tested the impact of 5 parameters on the localization accuracy: (1) translational shifts of the phantom, (2) rotational shifts of the phantom, (3) the CT slice thickness, (4) different anatomic sites, and (5) target shifts related to the body. For test 5, they used a plastic square with 5 BBs taped around its surface as the internal target. This virtual target was placed on the chamber holder of a Med Tec calibration water phantom. The chamber holder was moved in the vertical direction within the water phantom to simulate internal target shift.

The combination of IR camera-based ExacTrac auto setup and kV x-ray image based 3D autofusion method was used to localize the phantom to the corresponding isocenter. Two millimeter slice thickness was used for tests 1, 2, 4, and 5. The localization accuracy was evaluated by taking anterior/posterior (AP) and lateral portal films with the isocenter defined at the center of an implanted 2-mm-diameter BB. The results showed that for tests 1, 2, and 5, the localization accuracy was generally within 1 mm. For test 3, the localization accuracy between CT slice thickness of 2, 3, 4, and 5 mm varied little in the AP and lateral directions. The highest localization accuracy in the superior/inferior direction was

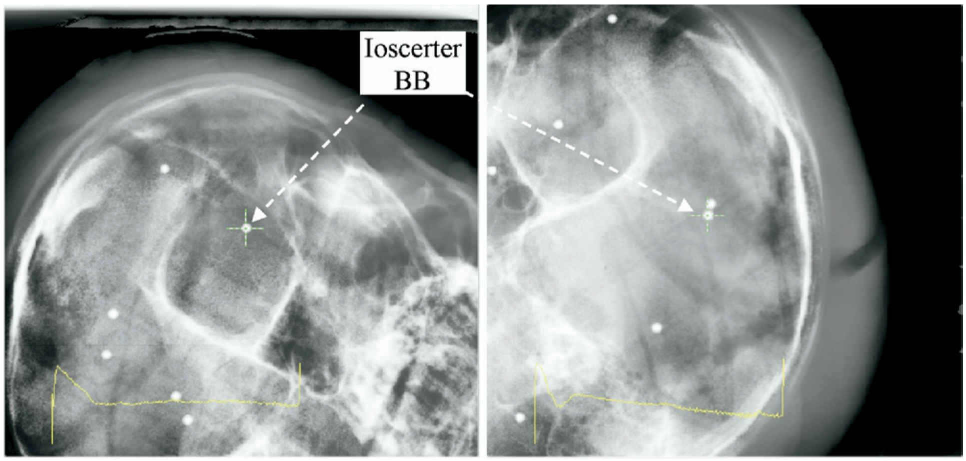

Fig. 5. Two verification kV x-ray images for evaluating the localization accuracy, which is determined by measuring the distance between the isocenter of the x-ray system (represented by the cross) and the treatment isocenter (represented by the center of the BB). The treatment isocenter seems to be excellently coincided with the x-ray system's isocenter in this pair of images. Only some of the 8 BBs are shown in the images due to limited view size.

achieved with the 2-mm slice thickness. For test 4, the localization accuracy in the head-and-neck region was better than in the thoracic and pelvis regions, most likely because the x-ray image quality was better.

Many factors have to be considered to interpret these results. The LINAC isocenter shifts slightly when the gantry rotates from the AP direction to a lateral direction. The agreement between the radiation isocenter and the isocenter defined by the wall-mounted lasers has a tolerance of about 0.7 mm, as demonstrated by the routine Winston-Lutz test. The evaluation method used in this study was not able to detect localization accuracy better than 0.7 mm; therefore, the observation that localization accuracy does not vary significantly with CT-slice thickness is likely due to a limitation of the evaluation method.

The results showed excellent localization accuracy for phantom with rotational shifts. This is because the phantom is a rigid object, and the external marker setup method could detect potential rotational shifts and made the correction. Clinically, a patient's contour can change between setup and simulation and the external markers may be placed in locations with motion resulting in rotational and translational errors during the first step of the positioning procedure. This study also tested the localization accuracy in a scenario where 1 of 5 internal markers was shifted 2 cm, and found that the localization accuracy was degraded to less than 1.5 mm.[42] This suggests that the 3D fusion localization method could not achieve desirable accuracy even in a rigid phantom if rotational and translational error existed when the x-rays were taken.

Recently, the 6D fusion localization software taking into account the rotational errors was clinically released. Jin *et al.*[43] have studied the accuracy of this localization method in a phantom. Eight BBs of 2-mm diameter were inserted into different locations of a head phantom. One of the BBs was used as the isocenter, while the rest of the BBs served as the implanted markers. Both 2- and 3-mm CT slices were studied. The head phantom was placed intentionally with certain rotational and translational shifts. Localization methods using 3D fusion, 6D fusion, and implanted markers were used. For both 3D and 6D fusions, the image areas with implanted BBs were excluded for the fusion. The localization methods were repeated 8 times at different locations, with the isocenter placed at the center of different BBs. Localization accuracy was evaluated using the portal film method reported by Yan *et al.*[42] The results from the implanted marker localization study were used as an additional standard to evaluate the 3D and 6D fusion methods. Figures 5 and 6 show a set of kV verification x-ray images and a set of MV portal film images, respectively, with the isocenter localized at the center of a BB.

Table 1 shows the average localization accuracy for 8 isocenters determined by the kV x-ray images and by the MV portal films, and for 2- and 3-mm slice thickness CT images. We note that both kV x-ray images and portal films demonstrated that excellent localization accuracy was achieved for all different isocenter locations using the 6D fusion method. Using 2- and 3-mm CT slice thickness seemed to produce no significant difference to the localization accuracy. This was consistent with the results from Yan *et al.*[42]

Table 2 gives the comparison of localization accuracy between the 3D fusion and 6D fusion methods at 2 different rotational settings and 2 different positions: the random position had about 3- to 5-cm translational deviations; the aligned position had no translational deviation. Rotational setting no. 1 and setting no. 2 had slightly different phantom

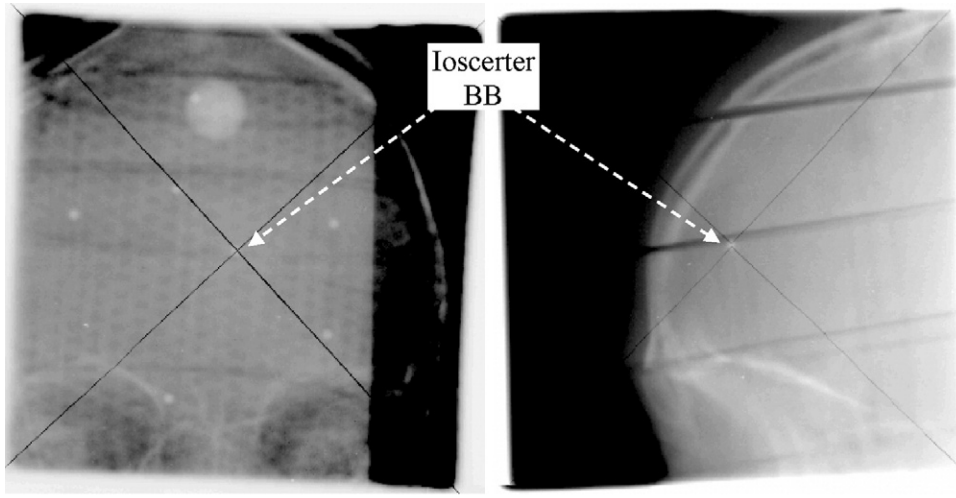

Fig. 6. AP and lateral MV portal images for evaluating the localization accuracy, which is determined by measuring the distance between the LINAC isocenter (center of the 9.8 × 9.8 cm portal represented by the intersection of 2 diagonal lines) and the treatment isocenter (represented by the center of the BB). Only some of the 8 BBs are shown in the images due to limited portal size.

rotational angles. The localization accuracy was evaluated by the implanted markers method.

We note that the 6D fusion localization had excellent accuracy for both angular settings, and for both the random and the aligned positions. In addition, the 3 angular deviations, determined by the 6D fusion method, had almost no variation for different isocenters and for different positions. However, for the 3D fusion method, there was a significant localization error, even at the aligned position. The localization error seemed to increase with the angular deviations. This is understandable because the isocenters were selected at the brain region, while the fusion was based on the bony structure, which was about 5 to 10 cm away from the isocenter. These results suggest that using 6D fusion could improve the localization accuracy for real patients compared with the 3D fusion method, especially when large rotational deviations exist at the initial setup when localization images were taken.

Patient studies for localization accuracy

Weiss *et al.*[44] evaluated the localization accuracy of the infrared body-marker–based ExacTrac system (without the x-ray component) in patients treated for gynecologic carcinomas, and compared it with patients positioned using the conventional room laser system. Patients were treated in a prone position. The electronic portal imaging device (EPID) was used for the evaluation. They found that there was no significant difference between the ExacTrac system and the room laser system. The localization error for the ExacTrac system ranged from −5.5 to 12.1, −14.4 to 7.3, and −4.1 to 15.6 mm at X, Y, and Z directions, respectively. This large localization uncertainty is understandable because patients were in the prone position. Respiratory motion in the abdominal region would transfer to the pelvis area. When the infrared markers were placed at locations of a patient with large movement, it seems that there was no any advantage of using the ExacTrac (infrared) system compared to using room laser system to align the patient to the isocenter tattoo. However, the ExacTrac system does offer the following benefits:

- Faster and automatic setup
- Motion tracking
- When the isocenter tattoo has to be marked at the location with large movement, the external markers can be placed at relative small motion locations to improve the localization repeatability and consistency
- Provides quantitative rotational errors
- Precisely controls the table position with the reference star attached to the table

Table 1. 6D fusion localization accuracy evaluated by verification kV x-ray images and MV portal images in an anthropomorphic head phantom with CT slice thickness of 2 and 3 mm

	By kV X-Rays			By MV Portal Film		
CT Slice Thickness	Image 1 (mm)	Image 2 (mm)	Overall	Image 1	Image 2	Overall
2 mm	0.42 ± 0.21	0.48 ± 0.18	0.57 ± 0.14	0.56 ± 0.19	0.60 ± 0.12	0.72 ± 0.12
3 mm	0.60 ± 0.13	0.56 ± 0.17	0.72 ± 0.16	0.60 ± 0.17	0.58 ± 0.21	0.74 ± 0.15

Table 2. Comparison of localization accuracy between 3D fusion and 6D fusion methods at 2 different rotational angles and 2 different translational positions

	3D Fusion (mm)		6D Fusion (mm)		Angles (degree)		
	Random Position	Aligned Position	Random Position	Aligned Position	α	β	γ
Setting 1	6.31 ± 1.20	2.44 ± 0.73	0.56 ± 0.18	0.57 ± 0.22	1.4 ± 0.1	1.8 ± 0.1	2.4 ± 0.1
Setting 2	3.55 ± 1.00	2.15 ± 0.99	0.62 ± 0.17	0.58 ± 0.21	1.6 ± 0.1	1.4 ± 0.1	0.53 ± 0.1

Yin *et al.* reported the localization accuracy for 25 spine patients using the combination of ExacTrac and 3D image fusion localization method.[45] The average accuracy for the 25 patients was reported to be 0.7 ± 0.7, 0.8 ± 0.9, and 0.9 ± 0.5 mm at anterior-posterior, left-right, and superior-inferior directions, respectively, with an overall average of 1.6 ± 0.9 mm. This result was consistent with the accuracy demonstrated in the phantom study. Note that the data were acquired and analyzed based on pseudo-rigid vertebral body with a stable patient immobilization device. The errors reported here for the portal films did not include linac isocenter inconsistency, which was in the order of about 0.7 mm, and the uncertainty of defining bony land markers in DRRs and portal films, especially for the MV portal films, which usually have poor image quality. The error defined was also strictly for the isocenter and did not include any deviations related to rotations around the isocenter.

Jin *et al.* have studied the localization accuracy of 6D fusion localization method in patients for both cranial and spinal lesions.[43,46] Verification kV x-ray images and MV portal film after localization were taken and compared to the corresponding DRRs. The bony structures were clearly seen in cranial kV x-ray images for all cranial patients. Both manual match and automatic 6D fusion match was used to evaluate the localization accuracy. Preliminary results suggested that about 1-mm localization accuracy could be achieved for the cranial patients. The 6D fusion localization method was also evaluated by comparing with the 3D fusion. The result in Fig. 7 shows the position difference calculated using 2 different image fusion techniques, 6D and 3D methods. It showed that there was up to a 4-mm difference between the 6D and the 3D localization methods. And the difference was correlated with the rotational shifts (up to 4° for the total angle) in the patient setup detected by the 6D fusion method. This suggests that rotational deviations indeed exist for real patients and the 6D fusion method could further improve the localization accuracy compared to the 3D fusion method.

Respiratory gating with real-time image guided verification

We have also recently tested the capabilities of the ExacTracGating system, a respiratory gating component added to the system. The effects of phantom speed, position of the gating window within the breathing cycle, systematic synchronization errors, and phantom rotations on the positioning and gating accuracy are included in the investigation. The accuracy of the ExacTracGating system is determined by comparing results obtained under gated conditions to those obtained under static non-gated conditions using the standard ExacTrac X-Ray 6D system.

Five lead BBs were embedded near the film plane of an IMRT verification phantom (MED-TEC, Orange City, IA) in a noncoplanar fashion to act as implanted fiducial markers for x-ray localization (Fig. 8). The phantom was placed on a platform capable of continuous 2D movement (Fig. 9), which has previously been described by Hugo *et al.*[23] A single CT set of the entire phantom was obtained using 3-mm slice thickness for planning. The platform remained motionless during the CT acquisition. A treatment isocenter was placed in one of the lead BBs located directly above the film plane and the CT planning data were exported to ExacTrac software, where fiducial lead BB positions were identified.

All field location measurements in this study were made by irradiating the phantom with a 5-mm-diameter SRS cone from a 0° gantry angle. Film was used to detect the delivered field positions by placing it in the coronal plane of the phantom just below the target lead BB. Measurements were restricted to the coronal plane. The major component of thoracic tumor motions is usually along the superior-inferior (S-I) direction[41] and accuracy in this dimension is easily measured from film placed in

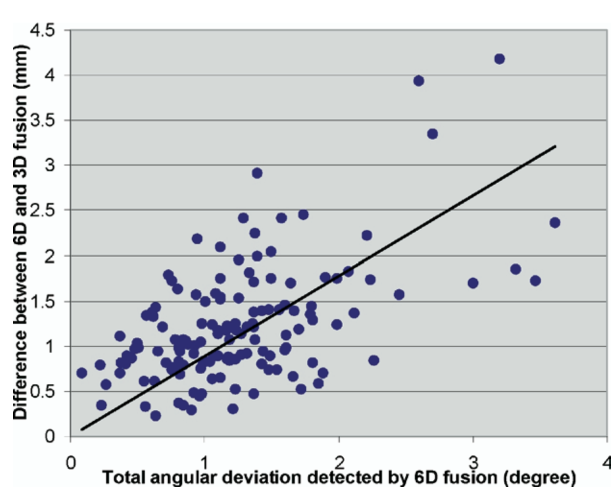

Fig. 7. Difference between 6D and 3D fusion methods vs. the total rotational angle detected by 6D fusion for patients initially set up with head mask-based stereotactic localization box.

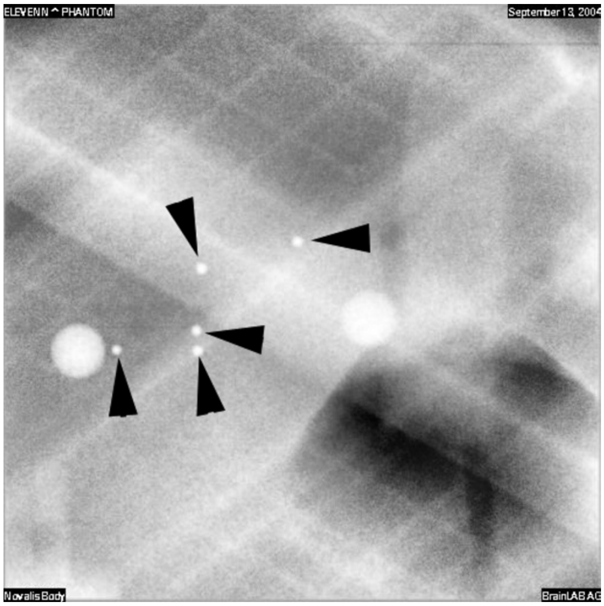

Fig. 8. X-ray image from one of the localization imaging units showing the 5 fiducial lead BBs implanted in the phantom. The larger circles in the image are the IR reflectors attached to the phantom surface.

the coronal plane. Five pins in the phantom mark the film and allow exposed films to be registered into a common reference frame for comparison. Field center or mass locations were used to determine accuracy.

The effect of phantom speed was investigated using 2 different 2D motions moving in the sagittal plane (Fig. 10). The first motion (10A) had a period of 5.7 seconds, an S-I range of 1.8 cm, and an A-P range of 1.2 cm. The second motion (10B) had the same displacement ranges as the first but had a shorter period of 3.6 seconds. Target position under gating conditions, represented by the position of the target BB in the film, was measured with gating levels of 10%, 50%, and 90% of the breathing trace peak-to-peak height, and was compared with the corresponding position under static condition. A symmetric gating window of 20% was placed around the gating level for every condition except for the 50% gating level and fast motion combination, for which a gating window of 30% was used. A 30% window was used for the specified condition because the beam-on time interval was too short for the LINAC to deliver any radiation using a 20% window. Fields gated at the 50% and 90% amplitude levels were not different from fields delivered under static conditions by more than one standard deviation (0.1 mm). Fields gated at 10% were offset by approximately 1 mm. This could be because much more radiation fluence was delivered to the target when it was below the 10% gating level than it was above this level (the target had the slowest motion speed when it was at the exhale peak).

Jin and Yin[24] have determined the overall system latency in a beta version of the ExacTracGating system

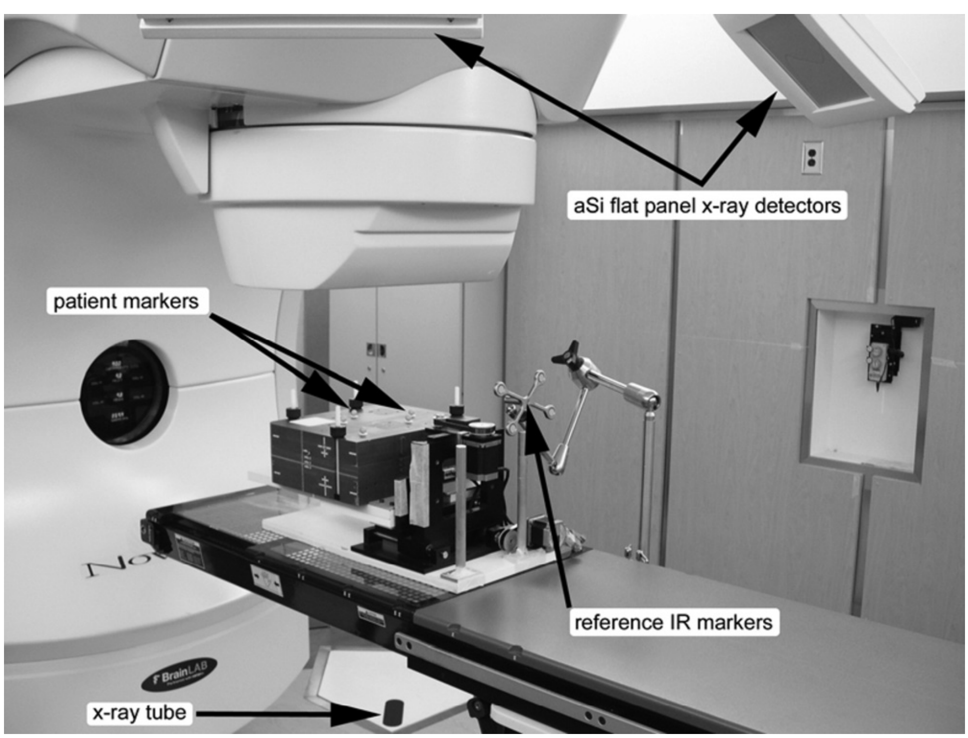

Fig. 9. The IMRT phantom can be seen resting on our mechanical motion platform. IR reflective patient and reference markers are attached to the phantom and the table, respectively. Ceiling-mounted aSi detectors and one of the floor-mounted x-ray tubes can be seen as well. All fields were delivered using our Novalis linac from the 0° gantry angle shown.

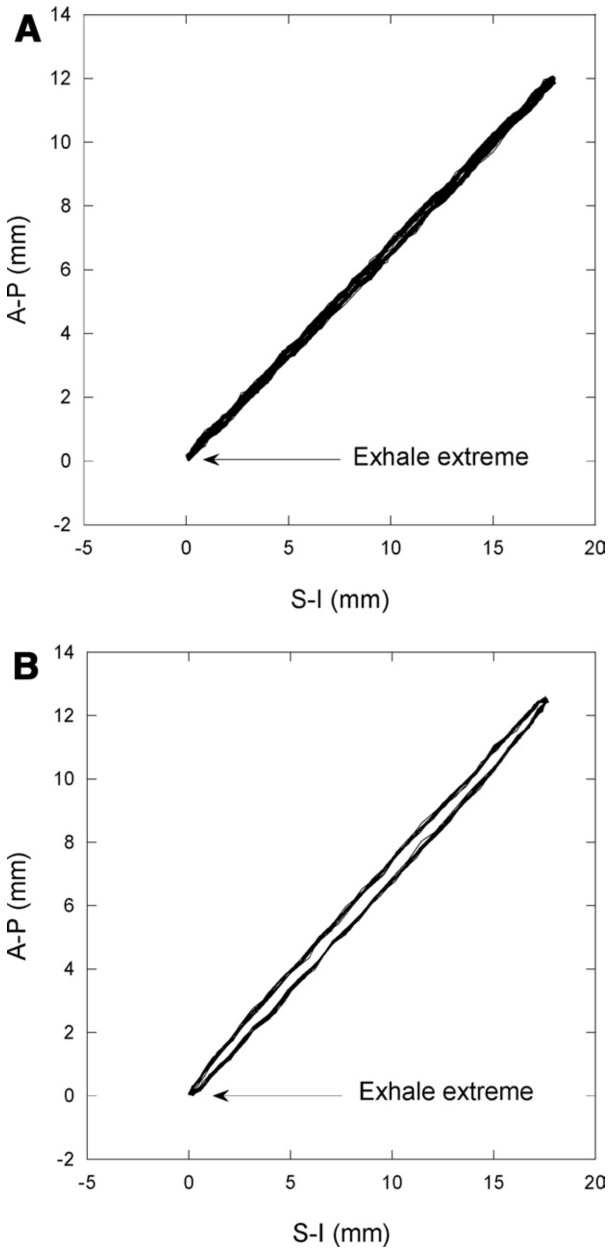

Fig. 10. (A) Slow and (B) fast phantom motion trajectories in the sagittal plane. The slow motion has a period of 5.7 seconds while the fast motion has a period of 3.6 seconds. Note the slightly larger amount of hysteresis in the fast motion.

by comparing the positions of a moving phantom in gated port films at multiple phases with the motion curve recorded by the IR cameras. A sampling frequency of 10 Hz was used for the IR system in the beta version. The phase offset between a motion curve generated from the gated port film data and the motion curve from the IR cameras showed an overall system delay of 0.17 ± 0.03 seconds.

We have measured this time delay in the ExacTrac-Gating system for the newly clinically released version, which uses 20-Hz sampling frequency. The clinical version also provides a LINAC latency parameter, which specifies a time in milliseconds by which ExacTracGating prematurely initiates the beam-on signal. The delay between system recognition of the phantom isocenter crossing the gating level and the start of irradiation was measured by varying this parameter. The centroid positions of fields delivered in the exhale only phase were compared with those delivered in both inhale and exhale phases using a series of increasing LINAC latency times. Fields gated in both phases are properly centered, although they may become elongated due to the offset of the field gated on inhale from the field gated on exhale side while exhale only fields with improper delay setting will be become offset in a given direction. The offset distance between exhale only and inhale and exhale fields was measured for 10, 50, 60, 70, and 100 millisecond LINAC latencies. The LINAC latency time at which the 2 fields coincide provides the correct value. Plotting the field offsets vs. LINAC latency time showed the system to have a LINAC delay of approximately 60 milliseconds. This system time delay was significantly less than 170 milliseconds measured at the beta version by Jin *et al.*[24], suggesting that the sampling time of the external marker's position by the IR system might be one of the main sources of the system time delay.

Although the ExacTracGating system component is not currently set up to correct for rotations of the implant markers, we have measured the effect of target rotation on the accuracy of gated localization and delivery in this system. Field locations were measured with the phantom rotated to 5°, 3°, −3°, and −5° around each of the three axes X, Y, and Z and compared to the field location with no rotation. The fast phantom motion was combined with a 90% gating level and 20% gating window for these field deliveries. All rotated fields remained within 0.5 mm of the field delivered to the non-rotated phantom.

DISCUSSION AND SUMMARY

The ExacTrac X-Ray 6D IGRT system uses multiple and integrated image modalities to achieve desired localization accuracy. The external marker and infrared camera based ExacTrac system could achieve excellent localization accuracy for the rigid object that has fixed relation between external markers and internal target. It also provides precise patient or couch positions. However, for patients with variable body shape/curvature, moveable surface, and non-fixed relation between external markers and internal structure, the internal target localization accuracy was poor if the ExacTrac system was used solely for setting up the patient. The 3D fusion method provided direct and automatic localization for internal bony structures. Excellent localization accuracy could be achieved for rigid bony structures when the patient was initially aligned with minimal rotational deviations. However, for real patients, considerable rotational offsets often exist when they were initially setup using the external markers. Therefore, accurate localization is often difficult to achieve in the real patients. The 6D fusion method took into account the potential angular difference between the x-ray images and the DRRs. An excellent localization accuracy was achieved for the anthropomorphic phantom, which was intentionally setup with certain rotational and translational deviations. Theoretically, for patients with target attached with rigid internal bony structures, such as patients with cranial and spinal lesions, the localization accuracy using 6D fusion should be as good as that in the phantom. Preliminary study seems to support this assumption.

The ExacTrac X-Ray 6D system uses kV x-ray to obtain 2D localization images with high spatial and contrast resolutions. The 6D fusion algorithm provides optimal match between the 2D localization images and the 3D CT simulation images. The infrared-based ExacTrac system provides precise control of patient positions and makes the accurate on-line adjustment of the patient position possible. In addition, the x-ray system is in fixed positions so that its isocenter is fixed and consistent with the linac isocenter defined by the room laser system. These make it an excellent IGRT system for targets attached to internal rigid bony structures, such as cranial and spinal lesions. In addition, it has the benefits of simple and fast operation, relatively low cost compared with other 3D image modalities, such as cone beam CT, and CT on-rail based systems. The radiation delivered to the patient during imaging is negligible compared to cone beam CT or 2D MV portal images.

It should be noted that the target localization accuracy of the ExacTrac X-Ray 6D IGRT system is dependent on the stability of localization object as well as the quality of 2D x-ray images and DRR images. For lesions that have motion related to the bony structures, an internal margin has to be applied to the target to form the internal target volume (ITV). This margin may be potentially reduced if gated treatment is applied using the ExacTracGating system for the real-time gating verification. On the other hand, the quality of x-ray images may not always optimal for image registration for large patients due to substantial overlapped structures and the special oblique configuration of the x-ray image devices. The path length of the x-rays in the patient's body is substantially larger compared to regular AP image. Although implant metal markers may minimize this problem, the addition of 3D tomographic imaging would be ideal to visualize anatomical structures for the purpose of accurate target localization.

REFERENCES

1. Fuss, M.; Salter, B.J.; Cavanaugh, S.X.; *et al.* Daily ultrasound-based image-guided targeting for radiotherapy of upper abdominal malignancies. *Int. J. Radiat. Oncol. Biol. Phys.* **59:**1245–56; 2004.
2. Lattanzi. J.; McNeeley, S.; Hanlon, A.; *et al.* Ultrasound-based stereotactic guidance of precision conformal external beam radiation therapy in clinically localized prostate cancer. *Urology* **55**: 73–8; 2000.
3. Ploeger, L.S.; Frenay, M.; Betgen, A.; *et al.* Application of video imaging for improvement of patient set-up. *Radiother. Oncol.* **68:**277–84; 2003.
4. Djajaputra, D.; Li, S. Real-time 3D surface-image-guided beam setup in radiotherapy of breast cancer. *Med. Phys.* **32:**65–75; 2005.
5. Keall, P.J.; Todor, A.D.; Vedam, S.S.; *et al.* On the use of EPID-based implanted marker tracking for 4D radiotherapy. *Med. Phys.* **31:**3492–9; 2004.
6. Beaulieu, L.; Girouard, L.M.; Aubin, S.; *et al.* Performing daily prostate targeting with a standard V-EPID and an automated radio-opaque marker detection algorithm. *Radiother. Oncol.* **73:**61–4; 2004.
7. Yin, F.F.; Ryu, S.; Ajlouni, M.; *et al.* Image-guided procedures for intensity-modulated spinal radiosurgery. Technical note. *J. Neurosurg.* **101**(Suppl 3):419–24; 2004.
8. Court, L.; Rosen, I.; Mohan, R.; *et al.* Evaluation of mechanical precision and alignment uncertainties for an integrated CT/LINAC system. *Med. Phys.* **30:**1198–210; 2003.
9. Cheng, C.W.; Wong, J.; Grimm, L.; *et al.* Commissioning and clinical implementation of a sliding gantry CT scanner installed in an existing treatment room and early clinical experience for precise tumor localization. *Am. J. Clin. Oncol.* **26:**e28–36; 2003.
10. Jaffray, D.A.; Siewerdsen, J.H.; Wong, J.W.; *et al.* Flat-panel cone-beam computed tomography for image-guided radiation therapy. *Int. J. Radiat. Oncol. Biol. Phys.* **53:**1337–49; 2002.
11. Sillanpaa, J.; Chang, J.; Mageras, G.; *et al.* Developments in megavoltage cone beam CT with an amorphous silicon EPID: Reduction of exposure and synchronization with respiratory gating. *Med. Phys.* **32:**819–29; 2005.
12. Pouliot, J.; Bani-Hashemi, A.; Chen, J.; *et al.* Low-dose megavoltage cone-beam CT for radiation therapy. *Int. J. Radiat. Oncol. Biol. Phys.* **61:**552–60; 2005.
13. Plathow, C.; Zimmermann, H.; Fink, C.; *et al.* Influence of different breathing maneuvers on internal and external organ motion: Use of fiducial markers in dynamic MRI. *Int. J. Radiat. Oncol. Biol. Phys.* **62:**238–45; 2005.
14. Rohlfing, T.; Maurer, C.R., Jr.; O'Dell, W.G.; *et al.* Modeling liver motion and deformation during the respiratory cycle using intensity-based nonrigid registration of gated MR images. *Med. Phys.* **31:**427–32; 2004.
15. Mah, D.; Freedman, G.; Milestone, B.; *et al.* Measurement of intrafractional prostate motion using magnetic resonance imaging. *Int. J. Radiat. Oncol. Biol. Phys.* **54:**568–75; 2002.
16. Ryu, S.; Khan, M.; Yin, F.F.; *et al.* Image-guided radiosurgery of head and neck cancers. *Otolaryngol. Head Neck Surg.* **130:**690–7; 2004.
17. Ryu, S.; Fang Yin, F.; Rock, J.; *et al.* Image-guided and intensity-modulated radiosurgery for patients with spinal metastasis. *Cancer* **97:**2013–8; 2003.
18. De Salles, A.A.; Pedroso, A.G.; Medin, P.; *et al.* Spinal lesions treated with Novalis shaped beam intensity-modulated radiosurgery and stereotactic radiotherapy. *J. Neurosurg.* **101**(Suppl 3): 435–40; 2004.
19. Jin, J.Y.; Yin, F.F.; Ryu, S.; *et al.* Dosimetric study using different leaf-width MLCs for treatment planning of dynamic conformal arcs and intensity-modulated radiosurgery. *Med. Phys.* **32:**405–11; 2005.
20. Wang, L.T.; Solberg, T.D.; Medin, P.M.; *et al.* Infrared patient positioning for stereotactic radiosurgery of extracranial tumors. *Comp. Biol. Med.* **31:**101–11; 2001.
21. Baroni, G.; Ferrigno, G.; Orecchia, R.; *et al.* Real-time three-dimensional motion analysis for patient positioning verification. *Radiother. Oncol.* **54:**21–7; 2000.
22. Hugo, G.D.; Agazaryan, N.; Solberg, T.D. The effects of tumor motion on planning and delivery of respiratory-gated IMRT. *Med. Phys.* **30:**1052–1066; 2003.
23. Hugo, G.D.; Agazaryan, N.; Solberg, T.D. An evaluation of gating window size, delivery method, and composite field dosimetry of respiratory-gated IMRT. *Med. Phys.* **29:**2517–25; 2002.
24. Jin, J.Y.; Yin, F.F. Time delay measurement for linac based treatment delivery in synchronized respiratory gating radiotherapy. *Med. Phys*. **32:**1293–6; 2005.
25. Berbeco, R.I.; Mostafavi, H.; Sharp, C.; *et al.* Tumor Tracking in the Absence of Radiopaque Markers. Proceedings of the 14th

International Conference on Computer Use in Radiation Therapy (ICCR). Seoul, South Korea; 2004.
26. Harada, T.; Shirato, H.; Ogura, S.; *et al.* Real-time tumor-tracking radiation therapy for lung carcinoma by the aid of insertion of a gold marker using bronchofiberscopy. *Cancer* **95:**1720–7; 2002.
27. Ozhasoglu, C.; Murphy, M.J. Issues in respiratory motion compensation during external-beam radiotherapy. *Int. J. Radiat. Oncol. Biol. Phys.* **52:**1389–99; 2002.
28. Shirato, H.; Harada, T.; Harabayashi, T.; *et al.* Feasibility of insertion/implantation of 2.0-mm-diameter gold internal fiducial markers for precise setup and real-time tumor tracking in radiotherapy. *Int. J. Radiat. Oncol. Biol. Phys.* **56:**240–7; 2003.
29. Whyte, R.I.; Crownover, R.; Murphy, M.J.; *et al.* Stereotactic radiosurgery for lung tumors: Preliminary report of a phase I trial. *Ann Thorac. Surg.* **75:**1097–10; 2003.
30. Ebe, K.; Shirato, H.; Hiyama, A.; *et al.* Integration of fluoroscopic real-time tumor-tracking system and tomographic scanner on the rail in the treatment room. *Int. J. Radiat. Oncol. Biol. Phys.* **60:**S604; 2004.
31. Vedam, S.S.; Kini, V.R.; Keall, P.J.; *et al.* Quantifying the predictability of diaphragm motion during respiration with a noninvasive external marker. *Med. Phys.* **30:**505–13; 2003.
32. Ahn, S.; Yi, B.; Suh, Y.; *et al.* A feasibility study on the prediction of tumour location in the lung from skin motion. *Br. J. Radiol.* **77:**588–96; 2004.
33. Hoisak, J.D.; Sixel, K.E.; Tirona, R.; *et al.* Correlation of lung tumor motion with external surrogate indicators of respiration. *Int. J. Radiat. Oncol. Biol. Phys.* **60:**1298–306; 2004.
34. Koch, N.; Liu, H.H.; Starkschall, G.; *et al.* Evaluation of internal lung motion for respiratory-gated radiotherapy using MRI: Part I--correlating internal lung motion with skin fiducial motion. *Int. J. Radiat. Oncol. Biol. Phys.* **60:**1459–72; 2004.
35. Liu, H.H.; Koch, N.; Starkschall, G.; *et al.* Evaluation of internal lung motion for respiratory-gated radiotherapy using MRI: Part II-margin reduction of internal target volume *Int. J. Radiat. Oncol. Biol. Phys.* **60:**1473–83; 2004.
36. Schweikard, A.; Shiomi, H.; Adler, J. Respiration tracking in radiosurgery *Med. Phys.* **31:**2738–41; 2004.
37. Tsunashima, Y.; Sakae, T.; Shioyama, Y.; *et al.* Correlation between the respiratory waveform measured using a respiratory sensor and 3D tumor motion in gated radiotherapy. *Int. J. Radiat. Oncol. Biol. Phys.* **60:**951–8; 2004.
38. Berbeco, R.I.; Nishioka, S.; Shirato, H.; *et al.* Residual motion of lung tumours in gated radiotherapy with external respiratory surrogates. *Phys. Med. Biol.* **50:**3655–67; 2005.
39. Plathow, C.; Zimmermann, H.; Fink, C.; *et al.* Influence of different breathing maneuvers on internal and external organ motion: Use of fiducial markers in dynamic MRI. *Int. J. Radiat. Oncol. Biol. Phys.* **62:**238–45; 2005.
40. George. R.; Ramakrishnan, V.; Siebers, J.; *et al.* Investigation of variables affecting residual motion for respiratory gated radiotherapy. *Med. Phys.* **32:**2124; 2005.
41. Seppenwoolde, Y.; Shirato, H.; Kitamura, K.; *et al.* Precise and real-time measurement of 3D tumor motion in lung due to breathing and heartbeat, measured during radiotherapy. *Int. J. Radiat. Oncol. Biol. Physz.* **53:**822–34; 2002.
42. Yan, H.; Yin, F.F.; Kim, J.H. A phantom study on the positioning accuracy of the Novalis Body system. *Med. Phys.* **30:**3052–60; 2003.
43. Jin, J.Y.; Ryu, S.; Faber, K.; *et al.* 2D/3D image fusion for accurate target localization and evaluation of a mask based stereotactic system in fractionated stereotactic radiotherapy of cranial lesions. *Med. Phys.* **33:**4557–66; 2006.
44. Weiss, E.; Vorwerk, H.; Richter, S.; *et al.* Interfractional and intrafractional accuracy during radiotherapy of gynecologic carcinomas: A comprehensive evaluation using the ExacTrac system. *Int. J. Radiat. Oncol. Biol. Phys.* **56:**69–79; 2003.
45. Yin, F.F.; Ryu, S.; Ajlouni, M.; *et al.* A technique of intensity-modulated radiosurgery (IMRS) for spinal tumors. *Med. Phys.* **29:**2815–22; 2002.
46. Jin, J.Y.; Ryu, S.; Rock, J.; *et al*. Image-guided target localization for stereotactic surgery: accuracy of 6D versus 3D image fusion. In: Kondziolka, D., ed. Radiosurgery (Vol. 6). Basel: Karger; 2006: 50-59.